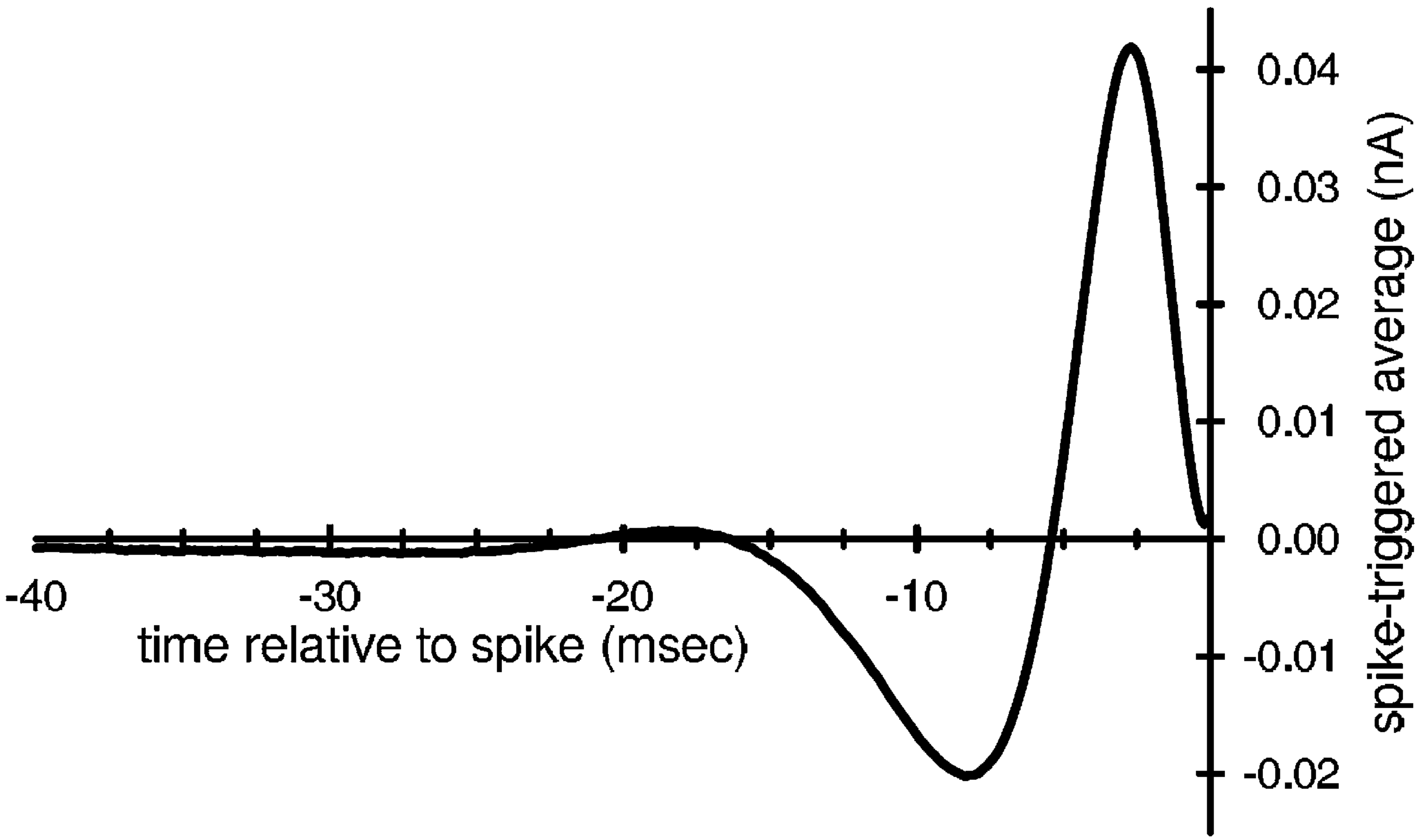

Aguera y Arcas, Fairhall and Bialek (Neural Computation 2003)

Lognormal firing rate distribution reveals prominent fluctuation–driven regime in spinal motor networks

Peter C Petersen, Rune W Berg

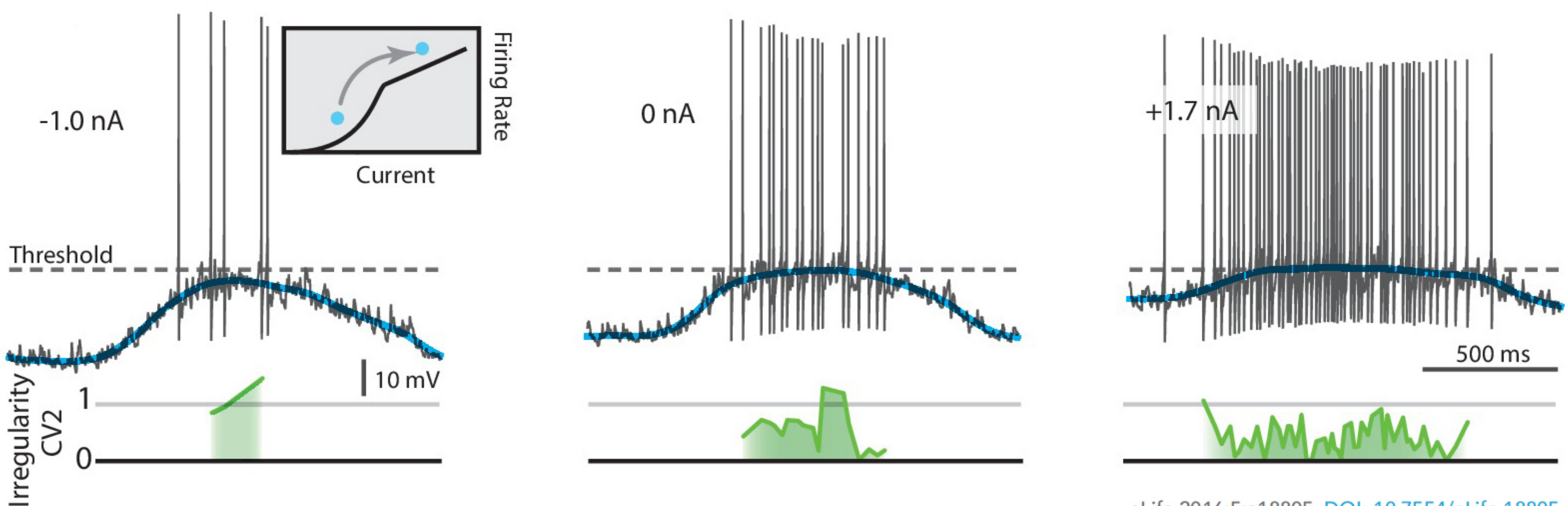

eLife 2016;5:e18805. DOI: 10.7554/eLife.18805

Correlating whisker behavior with membrane potential in barrel cortex of awake mice

Sylvain Crochet & Carl C H Petersen

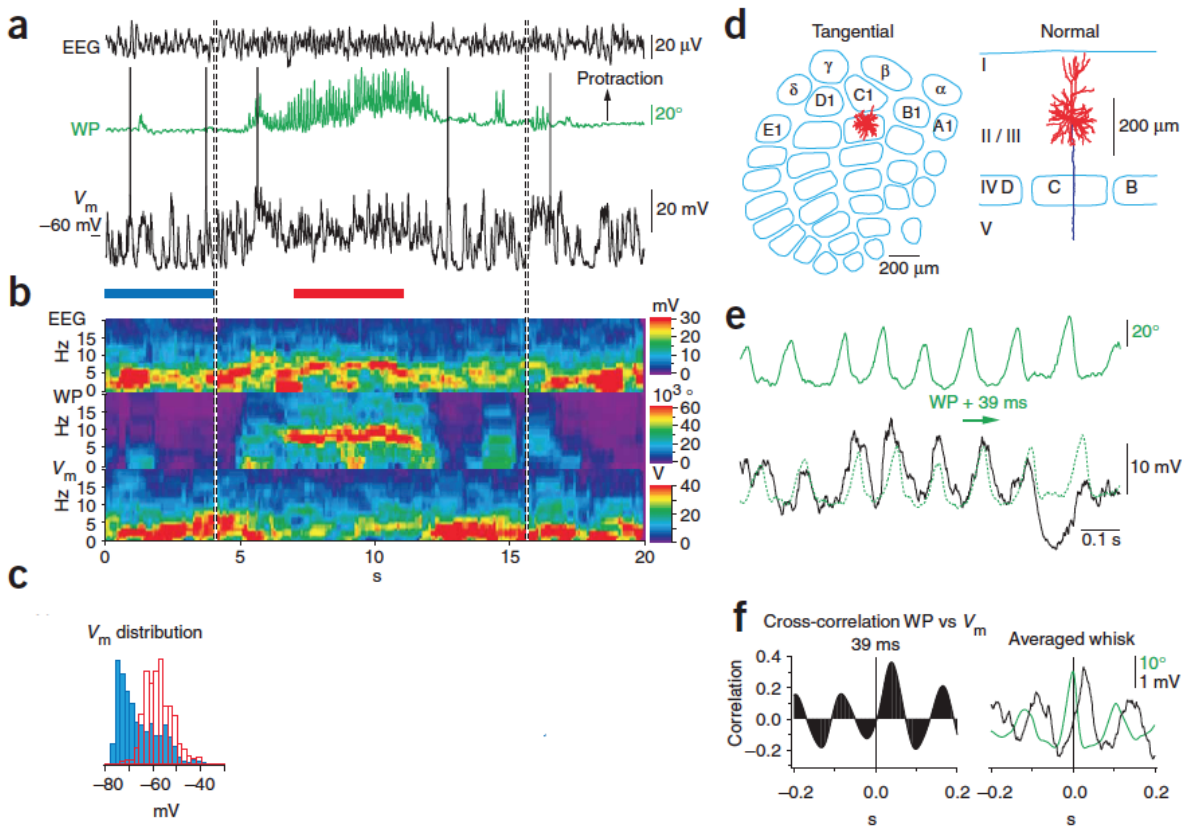

Figure 1 Membrane potential dynamics during whisker-related behavior. (**a**) Electroencephalogram (EEG) and whisker position (WP, green) were monitored during whole-cell recordings of membrane potential (V_m, black) from a layer 2/3 pyramidal neuron in the somatosensory barrel cortex of an awake mouse. Vertical dashed lines indicate periods of object contacts, which were removed for clarity. (Panels **a**–**f** all relate to this neuron.) (**b**) Sliding 1-s window fast Fourier transforms (FFT) of EEG, WP and V_m. (**c**) V_m distribution histograms, computed for the indicated epochs of quiet (blue) or whisking (red) behaviors. (**d**) Reconstructed dendrites (red) and descending primary axon (blue) within the barrel map (cyan). (**e**) V_m fluctuations and WP were correlated during whisking behavior. The WP (solid green line) shifted by 39 ms (dashed green line) revealed a close match with V_m (black line). (**f**) Both cross-correlation of WP with V_m (left) and whisker protraction–triggered V_m averaging (right) indicated robust phase locking.

The Journal of Neuroscience, May 15, 1998, *18*(10):3870–3896

The Variable Discharge of Cortical Neurons: Implications for Connectivity, Computation, and Information Coding

Michael N. Shadlen[1] **and William T. Newsome**[2]

[1]Department of Physiology and Biophysics and Regional Primate Research Center, University of Washington, Seattle, Washington 98195-7290, and [2]Howard Hughes Medical Institute and Department of Neurobiology, Stanford University School of Medicine, Stanford, California 94305

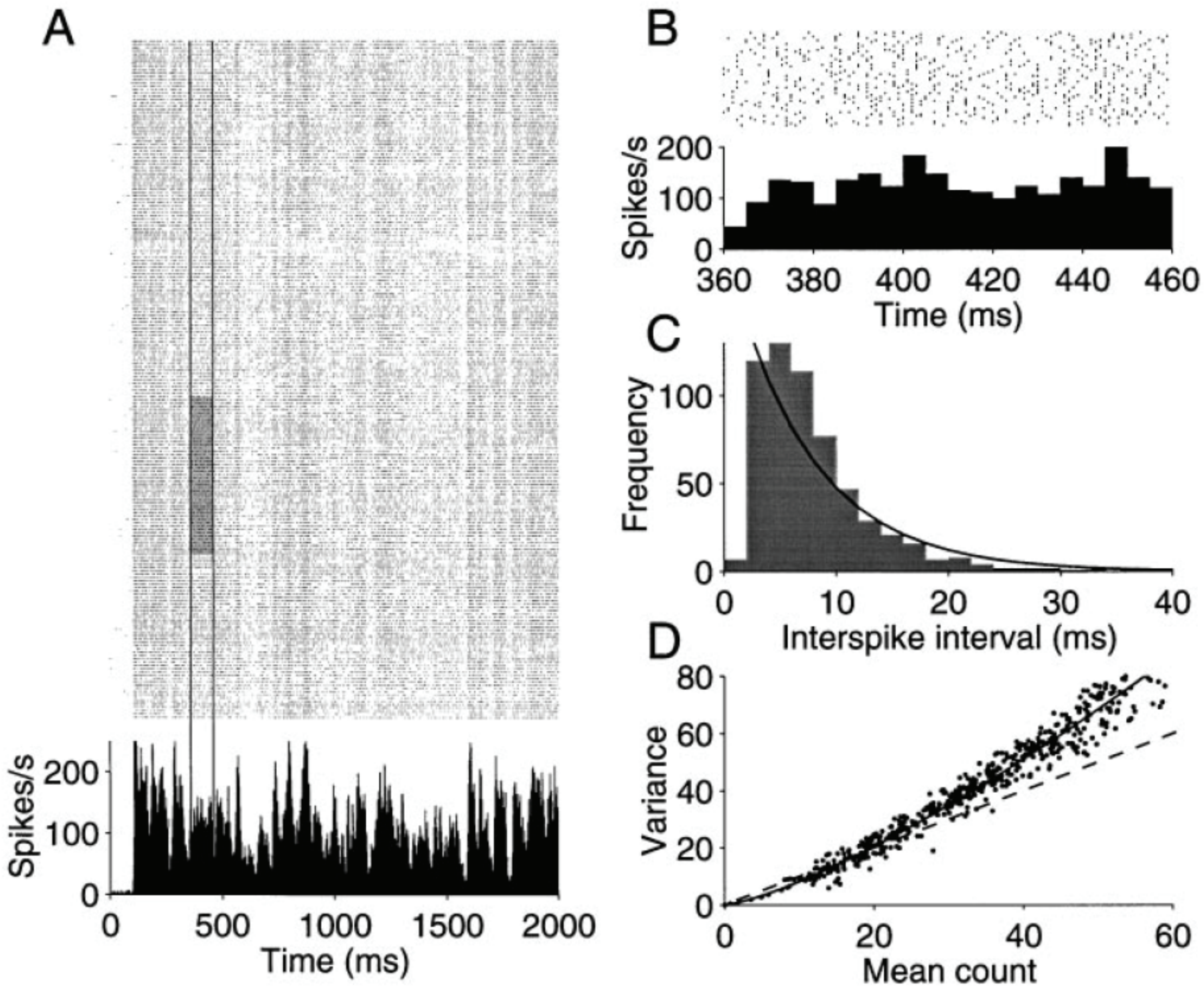

Figure 1. Response variability of a neuron recorded from area MT of an alert monkey. *A*, Raster and peristimulus time histogram (PSTH) depicting response for 210 presentations of an identical random dot motion stimulus. The motion stimulus was shown for 2 sec. Raster points represent the occurrence of action potentials. The PSTH plots the spike rate, averaged in 2 msec bins, as a function of time from the onset of the visual stimulus. The response modulates between 15 and 220 impulses/sec. *Vertical lines* delineate a period in which spike rate was fairly constant. The *gray region* shows 50 trials from this epoch, which were used to construct *B* and *C*. *B*, Magnified view of the shaded region of the raster in *A*. The spike rate, computed in 5 msec bins, is fairly constant. Notice that the magnified raster reveals substantial variability in the timing of individual spikes. *C*, Frequency histogram depicting the spike intervals in *B*. The *solid line* is the best fitting exponential probability density function. *D*, Variance of the spike count is plotted against the mean number of spikes obtained from randomly chosen rectangular regions of the raster in *A*. Each *point* represents the mean and variance of the spikes counted from 50 to 200 adjacent trials in an epoch from 100 to 500 msec long. The *shaded region* of *A* would be one such example. The best fitting power law is shown by the *solid curve*. The *dashed line* is the expected relationship for a Poisson point process.

The Journal of Neuroscience, April 1988, 8(4): 1172–1180

Spatially Opponent Excitation and Inhibition in Simple Cells of the Cat Visual Cortex

David Ferster

Department of Neurobiology and Physiology, Northwestern University, Evanston, Illinois 60208

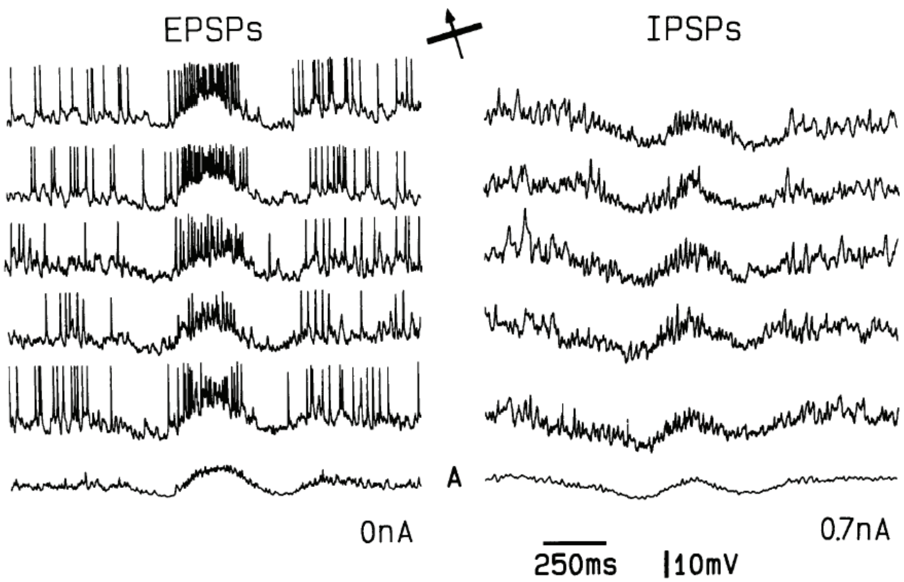

Figure 1. Intracellularly recorded responses of a simple cell evoked by a bright bar swept across its receptive field. The *inset* indicates the orientation and direction of motion of the stimulus. The *bar* measured 0.75° × 6° and traveled 4° in the 2 sec recorded in each trace. Whether EPSPs or IPSPs were visible in the records was controlled by the amount of current injected into the cell through the recording electrode. In this and all subsequent figures, the amount of current injected into the cell through the recording electrode while recording each set of traces is indicated to the *lower right*. EPSPs are shown to the *left* (0 nA), IPSPs to the *right* (0.7 nA). The *bottom trace* in each column (*A*) represents an average of 10 individual records.

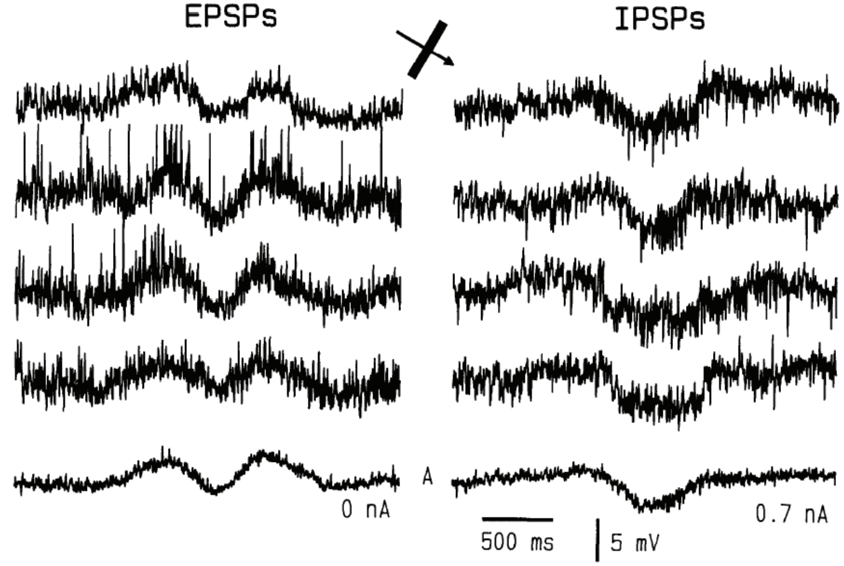

Figure 5. Responses to a moving bright bar recorded intracellularly from a second simple cell. The receptive field of this cell consisted of 2 ON regions flanking a central OFF region. The bar moved at a rate of 2°/sec.

Instantaneous Modulation of Gamma Oscillation Frequency by Balancing Excitation with Inhibition

Bassam V. Atallah[1,*] and Massimo Scanziani[2,*]

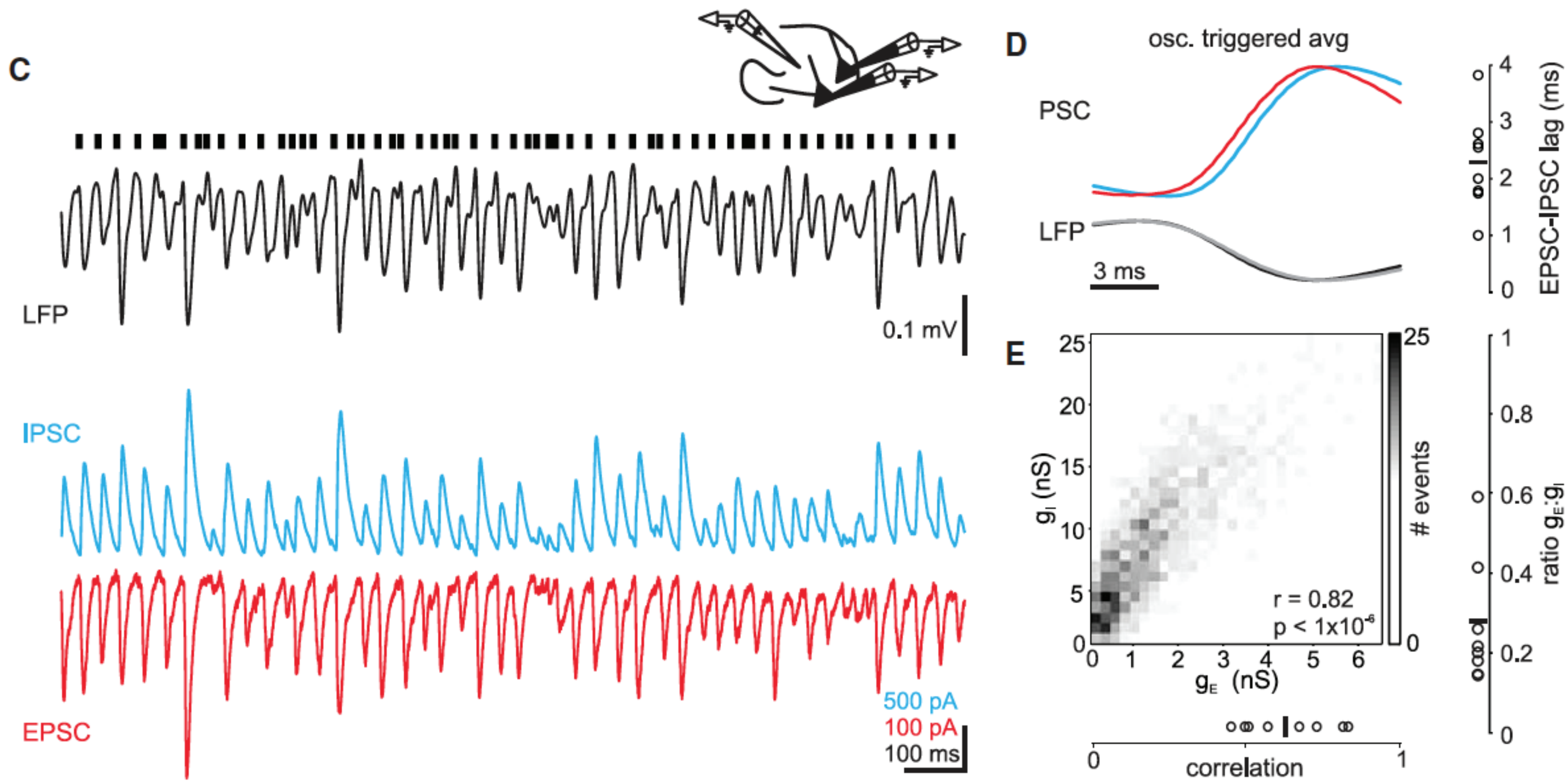

Figure 2. Excitation Instantaneously Balanced by Proportional Inhibition during Each Gamma Oscillation Cycle

(C) Dual patch-clamp recording from two neighboring CA3 pyramidal cells. Oscillations are monitored with an LFP electrode (black, positivity is up). EPSCs (red) and IPSCs (cyan) simultaneously recorded by holding two cells at the reversal potential for inhibition (−3 mV) and excitation (−87 mV), respectively. Note the correlated fluctuations in the amplitude of excitation and inhibition.

(D) (Left) Average time course of EPSC and IPSC (same cell as C) during an oscillation cycle recorded in the LFP, i.e., oscillation triggered average. EPSC is inverted for illustration purposes. LFPs recorded simultaneously with EPSCs and IPSCs are shown as black and gray traces, respectively. (Right) Summary of EPSC-IPSC lag during an oscillation cycle. Horizontal bar is the average.

(E) (Top) Cycle-by-cycle correlation between excitatory and inhibitory conductances recorded in the pair shown in (C). Summary of correlation between excitation and inhibition (bottom) and ratio of mean excitatory and inhibitory conductances (right) (n = 8 pairs). Vertical and horizontal bars illustrate respective averages.

The Journal of Neuroscience, April 26, 2006 • 26(17):4535–4545 • 4535

Behavioral/Systems/Cognitive

Neocortical Network Activity *In Vivo* Is Generated through a Dynamic Balance of Excitation and Inhibition

Bilal Haider, Alvaro Duque, Andrea R. Hasenstaub, and David A. McCormick
Department of Neurobiology, Kavli Institute for Neuroscience, Yale University School of Medicine, New Haven, Connecticut 06510

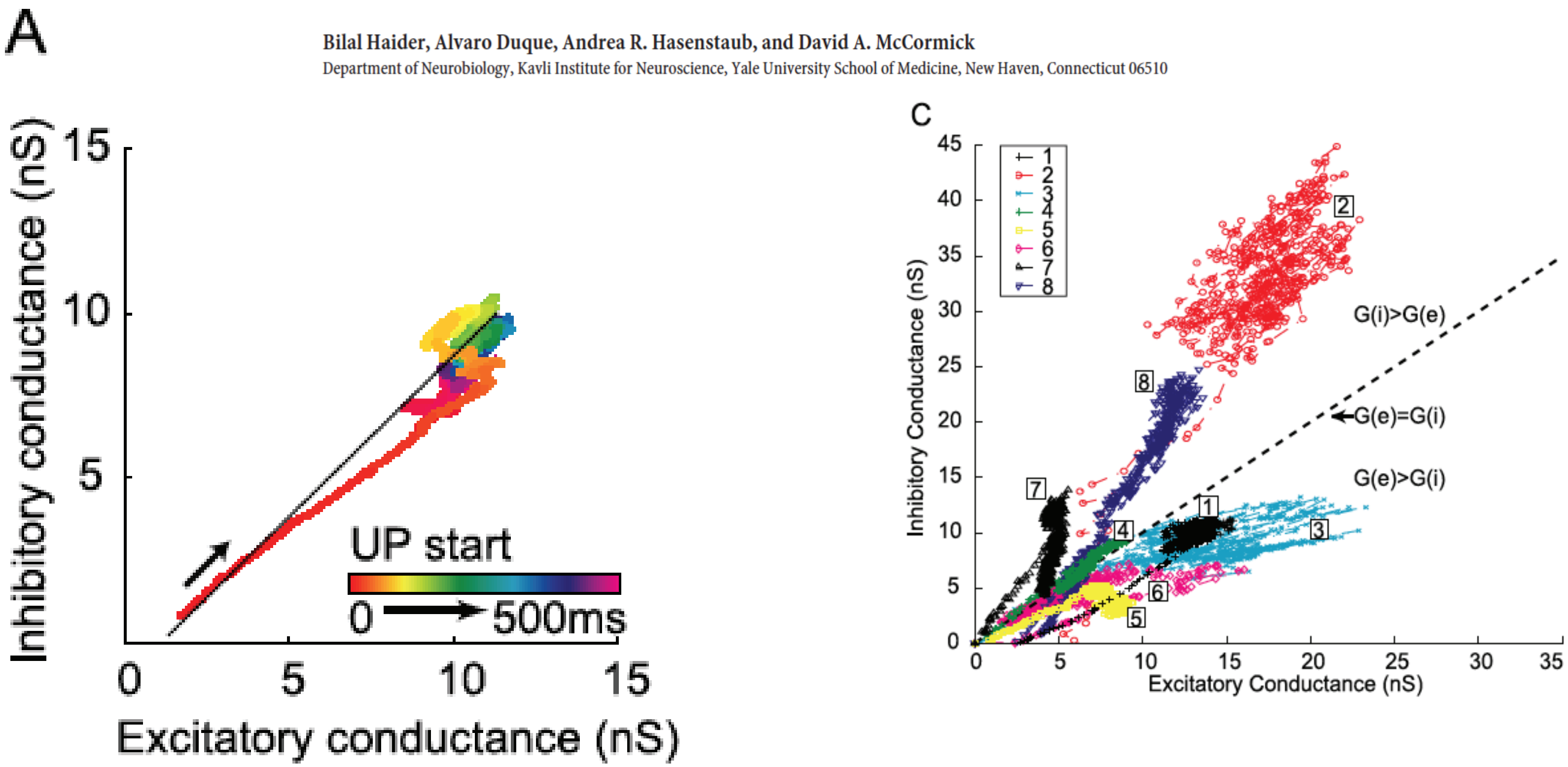

Figure 7. Excitatory and inhibitory conductances are proportional and balanced during Up states. ***A***, Plot of calculated excitatory and inhibitory conductances in a single neuron during the course of the Up state (0–500 ms, indicated by progressive movement through color bar) shows that excitation and inhibition remain proportional and nearly equal despite large changes in total conductance (slope of linear fit, $m = 0.98$; $r^2 = 0.78$). Note that the start of the Up state shows a deviation toward excitation, but rapidly swings toward inhibition and thereafter exhibits a balance between the two. ***C***, Excitation and inhibition are proportional and balanced both within and across neurons during recurrent network activity. Scatterplot of excitatory versus inhibitory conductances for a population of neurons ($n = 8$), calculated for 500 ms from the start of the Up state. Note the linear relationship for each individual neuron, as well as the clustering around a ratio of equal excitatory and inhibitory conductances ($G_e = G_i$; dashed line; 4 of 8 cells biased toward excitation, 3 of 8 cells toward inhibition, 1 of 8 cells approximately equal; population reversal potential, -37.2 ± 6.5 mV).

nature neuroscience

Synaptic scaling rule preserves excitatory–inhibitory balance and salient neuronal network dynamics

Jérémie Barral[1] & Alex D Reyes[1]

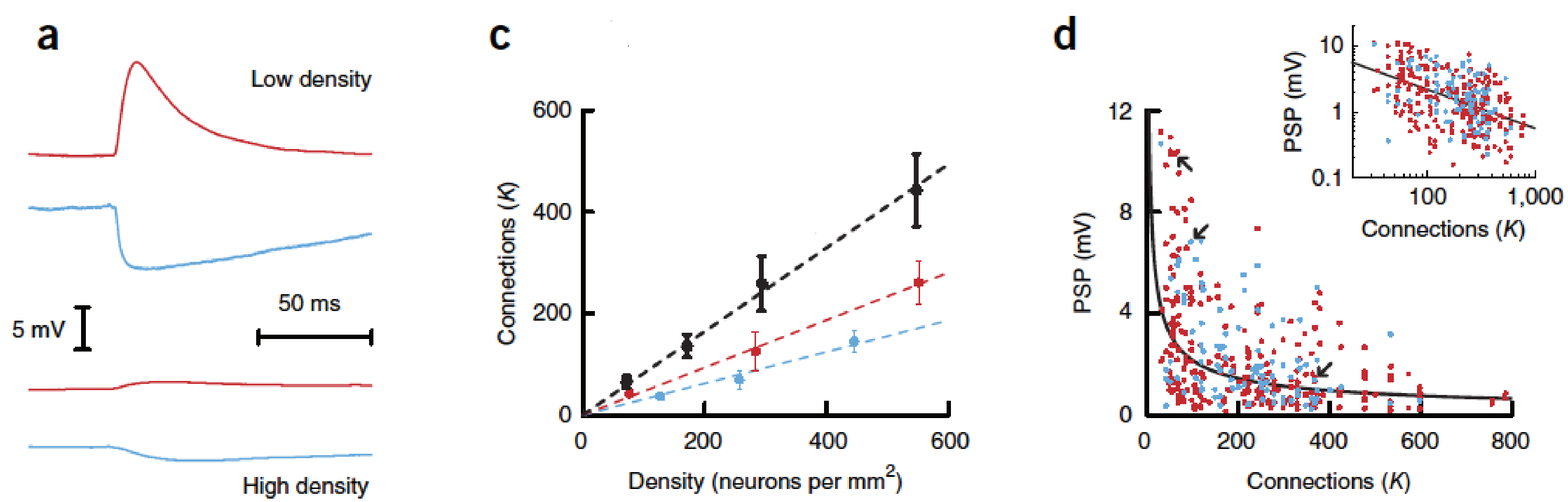

Figure 1 Synaptic scaling in networks of different sizes. (**a**) Representative E (red) and I (blue) PSPs in low and high density networks (arrows in **d**). (**c**) Number of connections (*K*) vs. density for E-to-E (red), I-to-E (blue) and total (black); s.d. calculated by bootstrapping data in **b**. (**d**) Amplitudes (*J*) of unitary EPSPs (red, $n = 261$) and IPSPs (blue, $n = 99$) vs. *K*. Inset: data in log–log scales. Slope of linear fit is –0.59.